



# Spectral, Thermal and Luminescent Properties of Nd<sup>3+</sup> Doped Borogerminate Glasses

S.L.Meena

Ceramic Laboratory, Department of Physics, Jai Narain Vyas University, Jodhpur, Rajasthan, India

**ABSTRACT:** Glass of the system  $(35-x)\text{GeO}_2:10\text{ZnO}:10\text{Li}_2\text{O}:10\text{CaO}:10\text{Na}_2\text{O}_3:10\text{WO}_3:15\text{B}_2\text{O}_3:x\text{Nd}_2\text{O}_3$  (where  $x=1, 1.5, 2$  mol %) have been prepared by melt-quenching method. The amorphous nature of the glasses was confirmed by X-ray diffraction studies. DTA curve was analysed to evaluate the glass transition temperature, crystallization temperature and melting temperature. Optical absorption spectra were recorded at room temperature for all glass samples. Slater-Condon parameters  $F_k$  ( $k=2, 4, 6$ ), Lande parameter  $\xi_{4f}$  and Racah parameters  $E^k$  ( $k=1, 2, 3$ ) have been computed. Using these parameters energies and intensities of these bands has been calculated. Judd-Ofelt intensity parameters  $\Omega_\lambda$  ( $\lambda=2, 4, 6$ ) are evaluated from the intensities of various absorption bands of optical absorption spectra. Using these intensity parameters various radiative properties like spontaneous emission probability ( $A$ ), branching ratio ( $\beta_R$ ), radiative life time ( $\tau_R$ ) and stimulated emission cross-section ( $\sigma_p$ ) of various emission lines have been evaluated.

**KEYWORDS:** ZLSLTBG Glasses, Thermal Properties, Judd-Ofelt Theory, Photoluminescence Properties.

## I. INTRODUCTION

Rare earth doped glasses are important materials as they find applications in white light emitting diodes, optoelectronics device, photonic technology, optical fiber amplifiers and thermal and mechanical sensors[1-5]. Among different ceramic glasses, germinate glasses have wide range applications in the field of glass ceramics with the advantage such as high density, high refractive index, high rare earth ions solubility and large third order nonlinear optical susceptibility [6-9]. Germinate glass is an extremely promising material for nonlinear applications, mechanical sensors, reflecting windows and laser in optics due to some of its essential characteristic features, such as low melting temperature, low phonon energy, low dispersion rates. They have high transparency and thermal stability [10-12]. Germinate glasses have excellent transparency, good physical, optical and mechanical properties. Borogerminate glass has low phonon energy, chemical and thermal stability [13,14]. Thus, it can be widely used in fiber amplifier and optical data storage devices. They present superior properties like that high transparency, low melting point, high gain density, high solubility for rare-earth ions. The host matrix compose of ZnO, a glass modifier/glass former a heavy metal oxide along with  $\text{Li}_2\text{O}$ ,  $\text{CaO}$ ,  $\text{Na}_2\text{O}$ ,  $\text{WO}_3$  and  $\text{B}_2\text{O}_3$ . The addition of CaO to the glass mixture improves the rare earth ion solubility leading to the possibility of using even higher concentrations of ions [15-18].

The present work reports on the thermal, absorption and emission properties of Nd<sup>3+</sup> doped zinc lithium sodalime tungsten borogerminate glass. The intensities of the transitions for the rare earth ions have been estimated successfully using the Judd-Ofelt theory, The laser parameters such as radiative probabilities ( $A$ ), branching ratio ( $\beta_R$ ), radiative life time ( $\tau_R$ ) and stimulated emission cross section ( $\sigma_p$ ) are evaluated using J.O. intensity parameters ( $\Omega_\lambda$ ,  $\lambda=2, 4$  and 6).

## II. EXPERIMENTAL TECHNIQUES

### Preparation of glasses

The following Nd<sup>3+</sup> doped borogerminate glass samples  $(35-x)\text{GeO}_2:10\text{ZnO}:10\text{Li}_2\text{O}:10\text{CaO}:10\text{Na}_2\text{O}_3:10\text{WO}_3:15\text{B}_2\text{O}_3:x\text{Nd}_2\text{O}_3$  (where  $x=1, 1.5, 2$ ) have been prepared by melt-quenching method. Analytical reagent grade chemical used in the present study consist of  $\text{GeO}_2$ ,  $\text{ZnO}$ ,  $\text{Li}_2\text{O}$ ,  $\text{CaO}$ ,  $\text{Na}_2\text{O}$ ,  $\text{WO}_3$ ,  $\text{B}_2\text{O}_3$  and  $\text{Nd}_2\text{O}_3$ . They were thoroughly mixed by using an agate pestle mortar. Then melted at 1075°C by an electrical muffle furnace for 2 hours. After complete melting, the melts were quickly poured in to a preheated stainless steel mould and annealed at temperature of 250°C for 2 h to remove thermal strains and stresses. Every time fine powder of cerium oxide was used for polishing the samples. The glass samples so prepared were of good optical quality and were transparent. The chemical compositions of the glasses with the name of samples are summarized in Table 1.

Table 1

Sample	Glass composition (mol %)
ZLSLTBG (UD)	35GeO <sub>2</sub> :10ZnO: 10Li <sub>2</sub> O: 10CaO: 10Na <sub>2</sub> O <sub>3</sub> : 10WO <sub>3</sub> : 15B <sub>2</sub> O <sub>3</sub>
ZLSLTBG ND(1.0)	34GeO <sub>2</sub> :10ZnO: 10Li <sub>2</sub> O: 10CaO: 10Na <sub>2</sub> O <sub>3</sub> : 10WO <sub>3</sub> : 15B <sub>2</sub> O <sub>3</sub> :1Nd <sub>2</sub> O <sub>3</sub>
ZLSLTBG ND(1.5)	33.5GeO <sub>2</sub> :10ZnO: 10Li <sub>2</sub> O: 10CaO: 10Na <sub>2</sub> O <sub>3</sub> : 10WO <sub>3</sub> : 15B <sub>2</sub> O <sub>3</sub> :1.5Nd <sub>2</sub> O <sub>3</sub>
ZLSLTBG ND(2.0)	33GeO <sub>2</sub> :10ZnO: 10Li <sub>2</sub> O: 10CaO: 10Na <sub>2</sub> O <sub>3</sub> : 10WO <sub>3</sub> : 15B <sub>2</sub> O <sub>3</sub> : 2Nd <sub>2</sub> O <sub>3</sub>

ZLSLTBG (UD) - Represents undoped zinc lithium sodalime tungsten borogerminate glass specimen.

ZLSLTBG (ND) - Represents Nd<sup>3+</sup> doped zinc lithium sodalime tungsten borogerminate glass specimens.

### III. THEORY

#### 3.1 Oscillator Strength

The intensity of spectral lines is expressed in terms of oscillator strengths using the relation [19].

$$f_{\text{expt.}} = 4.318 \times 10^{-9} \int \varepsilon(\nu) d\nu \quad (1)$$

where,  $\varepsilon(\nu)$  is molar absorption coefficient at a given energy  $\nu$  (cm<sup>-1</sup>), to be evaluated from Beer–Lambert law.

Under Gaussian Approximation, using Beer–Lambert law, the observed oscillator strengths of the absorption bands have been experimentally calculated [20], using the modified relation:

$$P_m = 4.6 \times 10^{-9} \times \frac{1}{cl} \log \frac{I_0}{I} \times \Delta\nu_{1/2} \quad (2)$$

Where  $c$  is the molar concentration of the absorbing ion per unit volume,  $l$  is the optical path length,  $\log I_0/I$  is optical density and  $\Delta\nu_{1/2}$  is half band width.

#### 3.2. Judd-Ofelt Intensity Parameters

According to Judd [21] and Ofelt [22] theory, independently derived expression for the oscillator strength of the induced forced electric dipole transitions between an initial  $J$  manifold  $|4f^N(S, L) J\rangle$  level and the terminal  $J'$  manifold  $|4f^N(S', L') J'\rangle$  is given by:

$$\frac{8\pi^2 m c \bar{\nu}}{3h(2J+1)n} \frac{1}{n} \left[ \frac{(n^2+2)^2}{9} \right] \times S(J, J') \quad (3)$$

Where, the line strength  $S(J, J')$  is given by the equation

$$S(J, J') = e^2 \sum_{\lambda=2, 4, 6} \Omega_{\lambda} \langle 4f^N(S, L) J \| U^{(\lambda)} \| 4f^N(S', L') J' \rangle^2 \quad (4)$$

In the above equation  $m$  is the mass of an electron,  $c$  is the velocity of light,  $\bar{\nu}$  is the wave number of the transition,  $h$  is Planck's constant,  $n$  is the refractive index,  $J$  and  $J'$  are the total angular momentum of the initial and final level respectively,  $\Omega_{\lambda}$  ( $\lambda=2, 4$  and  $6$ ) are known as Judd-Ofelt intensity parameters.

#### 3.3 Radiative Properties

The  $\Omega_{\lambda}$  parameters obtained using the absorption spectral results have been used to predict radiative properties such as spontaneous emission probability ( $A$ ) and radiative life time ( $\tau_R$ ), and laser parameters like fluorescence branching ratio ( $\beta_R$ ) and stimulated emission cross section ( $\sigma_p$ ).

The spontaneous emission probability from initial manifold  $|4f^N(S', L') J' \rangle$  to a final manifold  $|4f^N(S, L) J \rangle$  is given by:

$$A[(S', L') J'; (S, L) J] = \frac{64 \pi^2 \nu^3}{3h(2J'+1)} \left[ \frac{n(n^2+2)^2}{9} \right] \times S(J', \bar{J}) \quad (5)$$

$$\text{Where, } S(J', J) = e^2 [\Omega_2 \|U^{(2)}\|^2 + \Omega_4 \|U^{(4)}\|^2 + \Omega_6 \|U^{(6)}\|^2]$$

The fluorescence branching ratio for the transitions originating from a specific initial manifold  $|4f^N(S', L') J' \rangle$  to a final manifold  $|4f^N(S, L) J \rangle$  is given by

$$\beta[(S', L') J'; (S, L) J] = \sum_{S, L, J} \quad (6)$$

The radiative life time is given by

$$\tau_{rad} = \sum_{S, L, J} A[(S', L') J'; (S, L) J] = \quad (7)$$

Where, the sum is over all possible terminal manifolds. The stimulated emission cross-section for a transition from an initial manifold  $|4f^N(S', L') J' \rangle$  to a final manifold  $|4f^N(S, L) J \rangle$  is expressed as

$$\sigma_p(\lambda_p) = \left[ \frac{\lambda_p^4}{8\pi c n^2 \Delta\lambda_{eff}} \right] \times A[(S', L') J'; (\bar{S}, \bar{L}) J] \quad (8)$$

Where,  $\lambda_p$  the peak fluorescence wavelength of the emission band and  $\Delta\lambda_{eff}$  is the effective fluorescence line width.

### 3.4 Nephelauxetic Ratio ( $\beta$ ) and Bonding Parameter ( $b^{1/2}$ )

The nature of the R-O bond is known by the Nephelauxetic Ratio ( $\beta'$ ) and Bonding Parameters ( $b^{1/2}$ ), which are computed by using following formulae [23,24]. The Nephelauxetic Ratio is given by

$$\beta' = \frac{\nu_g}{\nu_a} \quad (9)$$

where,  $\nu_a$  and  $\nu_g$  refer to the energies of the corresponding transition in the glass and free ion, respectively. The values of bonding parameter  $b^{1/2}$  are given by

$$b^{1/2} = \left[ \frac{1-\beta'}{2} \right]^{1/2} \quad (10)$$

## IV. RESULT AND DISCUSSION

### 4.1. XRD Measurement

Figure 1 presents the XRD pattern of the samples shows no sharp Bragg's peak, but only a broad diffuse hump around low angle region. This is the clear indication of amorphous nature within the resolution limit of XRD instrument.

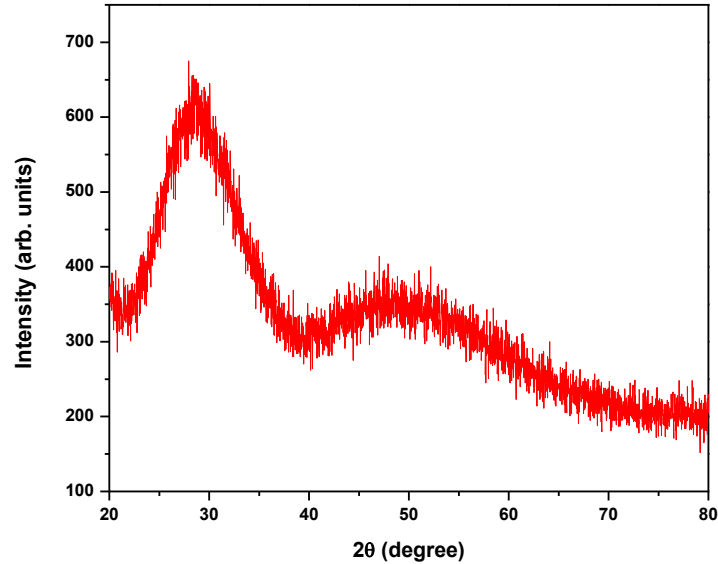


Fig.1: X-ray diffraction pattern of ZLSLTBG ND( 1.0) glass.

#### 4.2 Thermal Property

Differential thermal analysis checks the heat absorbed by glass samples during heating or cooling. Fig. 2 depicts the DTA thermogram of powdered ZLSLTBG ND(1.0) sample. The glass transition temperature ( $T_g$ ), onset crystallization temperature ( $T_c$ ), crystallization temperature ( $T_p$ ), melting temperature ( $T_m$ ), thermal stability ( $T_s$ ), Balaji Parameter ( $B_p$ ), Hurbe's criterion ( $H_R$ ) and reduced glass transition temperature ( $T_{rg}$ ) were calculated. Shankar's parameter also calculated by using eq. (15). All the determined thermal parameters are given in table 2.

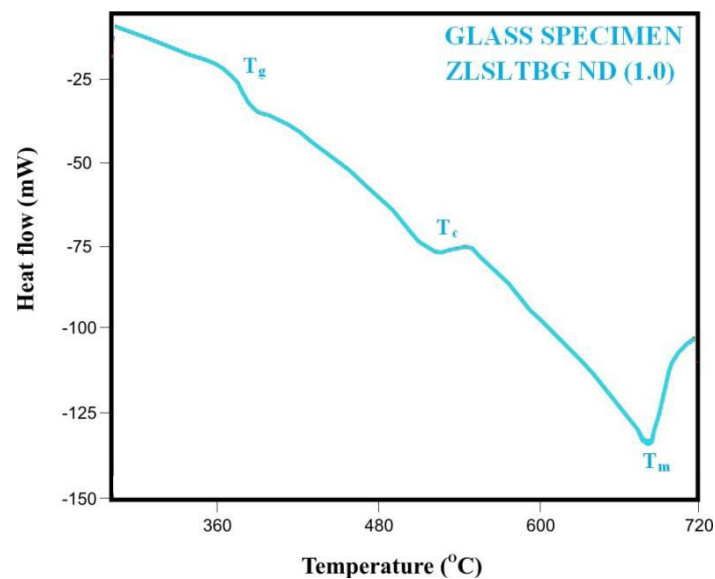


Fig.2: DTA curve of ZLSLTBG ND (1.0) glass.

Table 2 Thermal parameters determined from the DTA traces of ZLSLTBG ND glasses.

Sample Name	T <sub>g</sub> (°C)	T <sub>c</sub> (°C)	T <sub>p</sub> (°C)	T <sub>m</sub> (°C)	T <sub>s</sub> (°C)	B <sub>p</sub> (°C)	H <sub>R</sub> (°C)	K <sub>S</sub> (°C)	T <sub>rg</sub> (°C)
ZLSLTBG ND (1.0)	375	510	548	685	135	3.553	0.217	34.489	0.547
ZLSLTBG ND (1.5)	380	511	552	688	131	3.195	0.232	33.702	0.552
ZLSLTBG ND (2.0)	384	514	555	692	130	3.171	0.230	34.439	0.555

The thermal stability of the glass samples can be calculated by difference between onset crystallization temperature and transition temperature [25].

$$\text{Thermal Stability (T}_s\text{)} = T_c - T_g \quad (11)$$

Balaji Parameter can be calculated using [25].

$$\text{Balaji Parameter (B}_p\text{)} = [(T_c - T_g) / (T_p - T_c)] \quad (12)$$

Hruby's criterion is calculated using the Hurby's relation [25].

$$\text{Hruby's criterion (H}_R\text{)} = [(T_p - T_c) / (T_m - T_c)] \quad (13)$$

Reduced glass transition temperature is given as [25].

$$\text{Reduced glass transition temperature (T}_{rg}\text{)} = T_g / T_m \quad (14)$$

Thermal Parameter is given as [25].

$$K_S = [(T_m - T_c) (T_c - T_g) / T_m] \quad (15)$$

### 4.3. Absorption spectra

The absorption spectra of ZLSLTBG ND(1.0) glass, consists of absorption bands corresponding to the absorptions from the ground state <sup>4</sup>I<sub>9/2</sub> of Nd<sup>3+</sup> ions. Nine absorption bands have been observed from the ground state <sup>4</sup>I<sub>9/2</sub> to excited states <sup>4</sup>F<sub>3/2</sub>, <sup>4</sup>F<sub>5/2</sub>, <sup>4</sup>F<sub>7/2</sub>, <sup>4</sup>F<sub>9/2</sub>, <sup>2</sup>H<sub>11/2</sub>, <sup>4</sup>G<sub>5/2</sub>, <sup>4</sup>G<sub>7/2</sub>, <sup>4</sup>G<sub>9/2</sub>, and <sup>2</sup>G<sub>9/2</sub> for Nd<sup>3+</sup> doped ZLSLTBG ND( 1.0) glass.

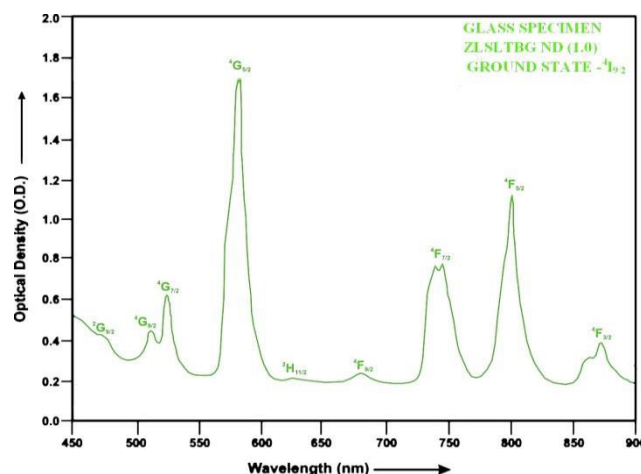


Fig.3: Absorption spectra of ZLSLTBG ND(1.0) glass.

The experimental and calculated oscillator strength for Nd<sup>3+</sup> ions in ZLSLTBG glasses are given in Table 3.

Table 3 Measured and calculated oscillator strength ( $P^m \times 10^{+6}$ ) of Nd<sup>3+</sup> ions in ZLSLTBG glasses.

Energy level from <sup>4</sup> I <sub>9/2</sub>	Glass ZLSLTBG ND(1.0)		Glass ZLSLTBG ND(1.5)		Glass ZLSLTBG ND(2.0)	
	P <sub>exp.</sub>	P <sub>cal.</sub>	P <sub>exp.</sub>	P <sub>cal.</sub>	P <sub>exp.</sub>	P <sub>cal.</sub>
<sup>4</sup> F <sub>3/2</sub>	3.45	3.45	3.42	3.44	3.38	3.42
<sup>4</sup> F <sub>5/2</sub>	8.35	8.34	8.30	8.30	8.24	8.26
<sup>4</sup> F <sub>7/2</sub>	9.48	9.79	9.42	9.74	9.38	9.72
<sup>4</sup> F <sub>9/2</sub>	0.64	0.52	0.62	0.52	0.60	0.51
<sup>2</sup> H <sub>11/2</sub>	0.25	0.15	0.22	0.15	0.19	0.15
<sup>4</sup> G <sub>5/2</sub>	24.36	24.61	23.45	23.72	22.55	22.84
<sup>4</sup> G <sub>7/2</sub>	4.28	4.98	4.22	4.91	4.18	4.84
<sup>4</sup> G <sub>9/2</sub>	2.25	2.17	2.22	2.16	2.17	2.15
<sup>2</sup> G <sub>9/2</sub>	0.97	2.76	0.95	2.75	0.92	2.73
r.m.s.deviation	0.6549		0.6590		0.6608	

Table4. Computed values of Slater-Condon, Lande, Racah, nephelauxetic ratio and bonding parameter for Nd<sup>3+</sup> doped ZLSLTBG glass specimens

Parameter	Free ion	ZLSLTBG ND(1.0)	ZLSLTBG ND(1.5)	ZLSLTBG ND(2.0)
F <sub>2</sub> (cm <sup>-1</sup> )	331.16	324.58	324.69	324.52
F <sub>4</sub> (cm <sup>-1</sup> )	50.71	50.72	50.70	50.74
F <sub>6</sub> (cm <sup>-1</sup> )	5.154	5.038	5.043	5.038
ξ <sub>4f</sub> (cm <sup>-1</sup> )	884.0	882.73	882.91	882.61
E <sup>1</sup> (cm <sup>-1</sup> )	5024.0	4947.12	4948.45	4947.09
E <sup>2</sup> (cm <sup>-1</sup> )	23.90	23.08	23.10	23.06
E <sup>3</sup> (cm <sup>-1</sup> )	497.0	489.58	489.56	489.54
F <sub>4</sub> /F <sub>2</sub>	0.1531	0.1563	0.1561	0.1564
F <sub>6</sub> /F <sub>2</sub>	0.0155	0.0155	0.0155	0.0155
E <sup>1</sup> /E <sup>3</sup>	10.1086	10.1048	10.1079	10.1057
E <sup>2</sup> /E <sup>3</sup>	0.0481	0.0471	0.0472	0.0471
β'		0.9958	0.9961	0.9959
b <sup>1/2</sup>		0.04578	0.04431	0.04552

The values of Judd-Ofelt intensity parameters are given in Table 5.

Table 5 Judd-Ofelt intensity parameters for Nd<sup>3+</sup> doped ZLSLTBG glass specimens.

Glass Specimen	Ω <sub>2</sub> (pm <sup>2</sup> )	Ω <sub>4</sub> (pm <sup>2</sup> )	Ω <sub>6</sub> (pm <sup>2</sup> )	Ω <sub>4</sub> /Ω <sub>6</sub>	Ref.
ZLSLTBG ND(1.0)	2.593	7.299	3.591	2.033	P.W.
ZLSLTBG ND(1.5)	2.297	7.282	3.572	2.039	P.W.
ZLSLTBG ND(2.0)	2.026	7.235	3.560	2.032	P.W.
ZLLVBM (ND)	2.876	7.830	3.393	2.308	[26].
SLBB (ND)	7.530	10.070	8.860	1.137	[27].
TBZN (ND)	1.574	2.368	1.768	1.339	[28].

#### 4.4. Excitation Spectrum

The Excitation spectra of ZLSLTBG ND (1.0) glass specimen has been presented in Figure 4 in terms of Excitation Intensity versus wavelength. The excitation spectrum was recorded in the spectral region 700–1000 nm fluorescence at 1065nm having different excitation band centred at 808 nm and 887 nm are attributed to the (<sup>4</sup>I<sub>9/2</sub>→<sup>4</sup>F<sub>5/2</sub>) and

( $^4I_{9/2} \rightarrow ^4F_{3/2}$ ) transitions, respectively. The highest absorption level is ( $^4I_{9/2} \rightarrow ^4F_{5/2}$ ) and is at 808 nm. So this is to be chosen for excitation wavelength.

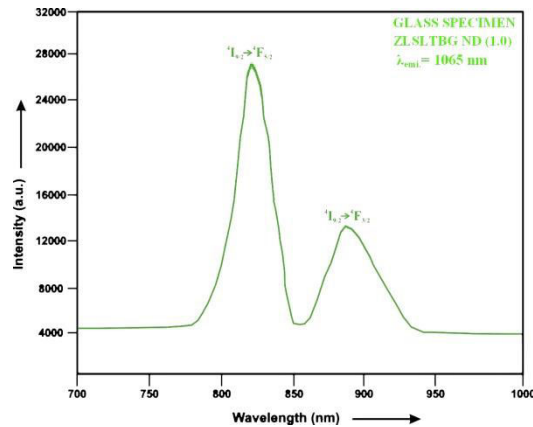


Fig.4: Excitation spectra of ZLSLTBG ND (1.0) glass.

#### 4.5. Fluorescence Spectrum

The fluorescence spectrum of  $Nd^{3+}$  doped in zinc lithium sodalime tungsten borogermanate is shown in Figure 5. There are six broad bands ( $^4G_{7/2} \rightarrow ^4I_{9/2}$ ), ( $^4G_{7/2} \rightarrow ^4I_{11/2}$ ), ( $^4F_{3/2} \rightarrow ^4I_{9/2}$ ), ( $^4F_{3/2} \rightarrow ^4I_{11/2}$ ), ( $^4F_{3/2} \rightarrow ^4I_{13/2}$ ) and ( $^4F_{3/2} \rightarrow ^4I_{15/2}$ ) respectively for glass specimens.

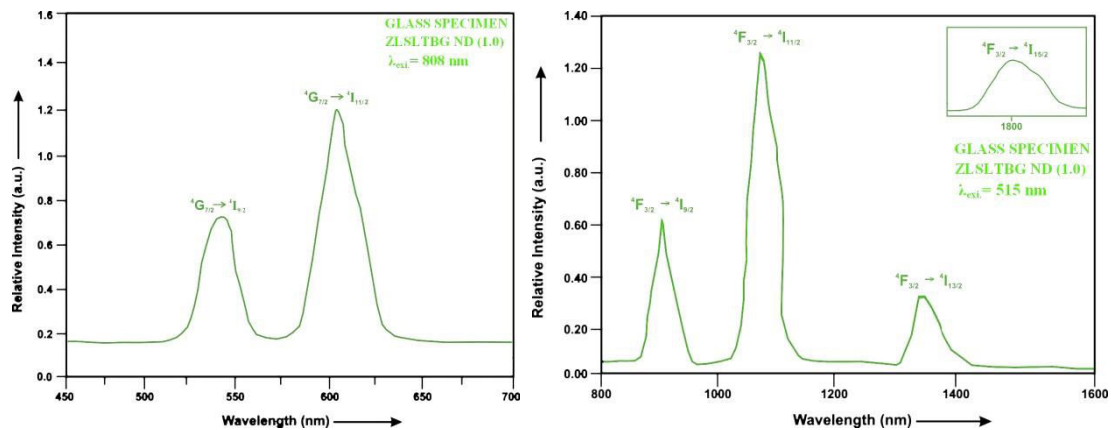


Fig.5: Fluorescence spectrum of ZLSLTBG ND(1.0) glass.

The wavelengths of these bands along with their assignments are given in Table 5.

**Table 6 Emission peak wave lengths ( $\lambda_p$ ), radiative transition probability ( $A_{rad}$ ), branching ratio ( $\beta_R$ ), stimulated emission crosssection ( $\sigma_p$ ), and radiative life time ( $\tau_R$ ) for various transitions in Nd<sup>3+</sup> doped ZLSLTBG glasses.**

Transit ion	ZLSLTBG ND( 1.0)				ZLSLTBG ND( 1.5)				ZLSLTBG ND(2.0)				
	$\lambda_{max}$ (nm)	$A_{rad}$ (s <sup>-1</sup> )	$\beta$	$\sigma_p$ (10 <sup>-20</sup> cm <sup>2</sup> )	$\tau_R$ (μs)	$A_{rad}$ (s <sup>-1</sup> )	$\beta$	$\sigma_p$ (10 <sup>-20</sup> cm <sup>2</sup> )	$\tau_R$ (μs)	$A_{rad}$ (s <sup>-1</sup> )	$\beta$	$\sigma_p$ (10 <sup>-20</sup> cm <sup>2</sup> )	$\tau_R$ (10 <sup>-20</sup> cm <sup>2</sup> )
<sup>4</sup> G <sub>7/2</sub> → <sup>4</sup> I <sub>9/2</sub>	53	2941	0.41	0.453	141.94	2900	0.4	0.471	145.58	2853	0.4	0.481	149.50
<sup>4</sup> G <sub>7/2</sub> → <sup>4</sup> I <sub>11/2</sub>	59	2862	0.40	1.140		2728	0.3	1.144		2599	0.3	1.185	
<sup>4</sup> F <sub>3/2</sub> → <sup>4</sup> I <sub>9/2</sub>	90	726.	0.10	0.745		725.	0.1	0.763		722.	0.1	0.786	
<sup>4</sup> F <sub>3/2</sub> → <sup>4</sup> I <sub>11/2</sub>	10	439.	0.06	2.108		438.	0.0	2.284		437.	0.0	2.469	
<sup>4</sup> F <sub>3/2</sub> → <sup>4</sup> I <sub>13/2</sub>	13	74.2	0.01	0.440		73.9	0.0	0.454		73.8	0.0	0.478	
<sup>4</sup> F <sub>3/2</sub> → <sup>4</sup> I <sub>15/2</sub>	18	1.77	0.00	0.026		1.77	0.0	0.026		1.77	0.0	0.027	

### V. CONCLUSION

In the present study, the glass samples of composition (35-x)GeO<sub>2</sub>:10ZnO: 10Li<sub>2</sub>O: 10CaO: 10Na<sub>2</sub>O<sub>3</sub>: 10WO<sub>3</sub>: 15B<sub>2</sub>O<sub>3</sub>: xNd<sub>2</sub>O<sub>3</sub>. (where x =1, 1.5, 2 mol %) have been prepared by melt-quenching method. The large value of Balaji parameter indicate that the prepared glass samples have good thermal stability. The stimulated emission cross section ( $\sigma_p$ ) has highest value for the transition (<sup>4</sup>F<sub>3/2</sub>→<sup>4</sup>I<sub>11/2</sub>) in all the glass specimens doped with Nd<sup>3+</sup> ion. This shows that (<sup>4</sup>F<sub>3/2</sub>→<sup>4</sup>I<sub>11/2</sub>) transition is most probable transition. The results show that the Nd<sup>3+</sup> doped germinate glasses could be potential candidates for photonic and laser devices.

### REFERENCES

- [1]. Meena,S.L.(2026).Spectral and Thermal Properties of Dy<sup>3+</sup> ions doped Phosphate Glasses for White LED Technology,Int.J.Inno.Res.Sci.Eng.Tech.15,9580-9587.
- [2].Matos,I.M.,Balzaretto, N.M.(2024).Effect of mixed alkali ions on the structural and spectroscopic properties of Nd<sup>3+</sup> doped silicate glasses,Res.Mat.21,100517,1-8.
- [3].Meena, S.L.(2026).Spectral, Thermal and Raman analysis of Tm<sup>3+</sup> doped in phosphate glasses for optical temperature sensor applications, IOSR Appl.Phys.18,42-30.
- [4]. Babu,K.V.,Cole,S.(2018).Luminescence properties of Dy<sup>3+</sup> doped alkali lead alumino borosilicate glasses,Ceram.Int.9080-9090.
- [5]. De,M.,Jana,S.(2020).Optical characterization of Eu<sup>3+</sup> doped titanium barium lead phosphate glass,Optik-Int.J.for light and Elect.Opt.215,164718,1-7.
- [6].Lemiere,A.,Bondzior,B.,Kuusela,L.,Veber,A.,Petit,L.(2023).Spectroscopic properties of Er<sup>3+</sup> doped germinate glasses before and after a heat treatment process,Opt.Mat.Exp.13,218-228.
- [7].Bondzior,B.,Lisiecki,R.(2024).Excellent Color Purity and Luminescence Thermometry Performance in Germanate Tellurite Glass Doped with Eu<sup>3+</sup>,Appl.Sci.14,1-15.
- [8]. Meena,S.L.(2020).Spectral and Thermal Properties of Eu<sup>3+</sup> ions doped Zinc Lithium AluminoAntimony Borogermanate Glasses,Int.J.Eng. Sci.Inv.9,10-16.
- [9].Yasukevich,A.S.,Dunia,G.,Kisel,V.E.E.,Kuleshov,N.V.(2020).Spectral luminescence properties of oxyfluoride lead silicate germinate glasses ,J.Lumin.229,117667.
- [10].Elan,F.,FalcaoFilho,E.L.,Camilo,M.E.Garcia,J.A.M.,Kassab,L.R.P.,Arujo,C.B.(2016).Up-conversion photoluminescence in GeO<sub>2</sub>-PbO glass codoped with Nd<sup>3+</sup> and Yb<sup>3+</sup>,Opt.Mater 60,313-317.

- [11].Meena,S.L.(2026). Spectral,Transmittance and Thermal analysis of Tb<sup>3+</sup> doped ytterbium zinc lithium calcium tungsten borogermanate glasses,IOSR Appl.Phys.18,31-38.
- [12].Guan,P.,Fan,X.,Li,W.,Liu,X.,Yu,C.Zhang,L.,Hu,L.(2016).High efficiency 2 μm laser in a single-mode Tm-doped lead germanate composite fiber,Chin.Opt.Lett.14,72-75.
- [13]. Meena,S.L.(2021). Spectral and Thermal Properties of Sm<sup>3+</sup>Doped in Zinc Lithium Alumino Antimony Borogermanate Glasses, Int.J.Inno.Res.Sci.Eng.Tech.10,1107-14.
- [14].Watekar,P.R.,Ju,S.,Han,W.T.(2008).Optical properties of Ho<sup>3+</sup>doped alumino-germano-silica glass optical fiber,J.Non-Cryst.Solids,254,1435-1459.
- [15].Cao,W.,Huang,F.,Wang,T.,Ye,R.,Lei,R.,Tian,Y.,Zhang,J.,Xu,S.(2018).2.0μm emission of Ho<sup>3+</sup> doped germane silicate glass sensitized by non-rare earth ion Bi: a new choice for 2.0 μm laser,Opt.Mater,75,695-698.
- [16].Meena,S.L.(2022). Spectral and Upconversion Properties of Eu<sup>3+</sup>Doped in Zinc Lithium Cadmium Alumino Borogermanate Glasses, Int. J. Inno. Res. Sci. Eng. Tech. 11, 1675-81.
- [17].Zhou,D.,Jin,D.,Ni,Q.,Song,X.,Bai,X.Han,K.(2019).Fabrication of double-cladding Ho<sup>3+</sup>/Tm<sup>3+</sup> co-doped Bi<sub>2</sub>O<sub>3</sub>-GeO<sub>2</sub>-Ga<sub>2</sub>O<sub>3</sub>-BaF<sub>2</sub> glass fiber and its performance in a 2.0μm laser,J.Am.Ceram.Soc.102,4748-4756.
- [18].Golonku,H.,Ohishi,Y.(2005).Spectroscopic properties of Er<sup>3+</sup> doped PbO-Ga<sub>2</sub>O<sub>3</sub>-GeO<sub>2</sub> glass for optical amplifiers,Opt.Mater,27,679-690.
- [19].Meena,S.L.(2021). Spectral and Thermal and Raman Analysis of Tm<sup>3+</sup> doped in phosphate glasses for optical temperature sensor applications,IOSR Appl.Phys.18,24-30.
- [20].Meena,S.L.(2021). Spectral and Raman Analysis of Er<sup>3+</sup> doped Zinc Lithium Antimony Sodalime Tellurite Glasses,Int.J.Eng.Sci.Inv.10,09-15.
- [21].Judd, B.R. (1962). Optical Absorption Intensities of Rare Earth Ions. Physical Review, 127, 750.
- [22]. Ofelt, G.S. (1962). Intensities of Crystal Spectra of Rare Earth Ions. The J. Chem. Phys., 37, 511.
- [23]. Sinha, S.P. (1983). Systematics and properties of lanthanides, Reidel, Dordrecht.
- [24]. Krupke, W.F. (1974).IEEE J. Quantum Electron QE, 10,450.
- [25].Meena,S.L.(2025).Spectral, Thermal and Photoluminescence Analysis of Phosphate Glasses with Trivalent Holmium for 2.0 μm optoelectronic applications, IOSR Appl.Phys.18,01-08.
- [26].Meena,S.L.(2020).Spectral and Transmittance properties of Nd<sup>3+</sup> ions doped zinc lithium lead vanadium boromolybdate glasses, IOSR Appl.Phys.12,01-06.
- [27].Rajesh,D.,Balakrishna,A.,SEshadri,M.,Ratnakaram,Y.C.(2012).Spectroscopic investigations on Pr<sup>3+</sup> and Nd<sup>3+</sup> doped strontium lithium bismuth borate glasses,Mol.Bio.Mol.Spect.97,963-974.
- [28].Marzuki,A.,Pramuda,A.,Fausta,D.E.(2020).Effect of Nd<sub>2</sub>O<sub>3</sub> and Na<sub>2</sub>O concentration on physical and spectroscopic properties of TeO<sub>2</sub>-Bi<sub>2</sub>O<sub>3</sub>-ZnO-Na<sub>2</sub>O-Nd<sub>2</sub>O<sub>3</sub> glasses,Matter.Res.Express,7,065201.



INTERNATIONAL  
STANDARD  
SERIAL  
NUMBER  
INDIA



# INTERNATIONAL JOURNAL OF INNOVATIVE RESEARCH

IN SCIENCE | ENGINEERING | TECHNOLOGY

 9940 572 462  6381 907 438  [ijirset@gmail.com](mailto:ijirset@gmail.com)



[www.ijirset.com](http://www.ijirset.com)

Scan to save the contact details